Vol. 39 (2008) ACTA PHYSICA POLONICA B No 9

LOW-x FINAL STATES AT HERA*

Christian Kiesling

Max-Planck-Institute for Physics, Munich, Germany

(Received May 12, 2008)

In this lecture we present data on hadronic final states from electron–proton reactions at low Bjorken x, taken by the two colliding beam experiments H1 and ZEUS at HERA. The data are discussed in the context of a variety of QCD-based models, which allow for a detailed study of the QCD dynamics in the production of partons and their fragmentation into hadrons. The HERA data fully support the perturbative approach of the DGLAP evolution scheme, although some hints may be visible in certain kinematic regions for the need of alternative formulations, such as BFKL dynamics.

PACS numbers: 13.60.Hb, 13.87.Ce, 13.87.Fh, 12.38.Qk

1. Introduction

Deep inelastic scattering (DIS) of charged leptons on protons and nuclei has been an essential tool to uncover the inner structure of hadrons. The electron–proton collider HERA, unique in the world, has been the ideal place for more than 15 years to study DIS with electron and positron beams, colliding head-on with protons. On June 30, 2007, at 23:00, the HERA collider was shut down for good, ending an extremely successful period of data taking with the two colliding beam experiments H1 [1] and ZEUS [2].

The subject of this lecture is to focus on details of the hadronic final states at low Bjorken x from electron (positron)–proton reactions at HERA. DIS reactions sensitively probe the strong interactions of quarks and gluons ("partons") in the kinematic regime of large momentum transfer Q^2, *e.g.* by measuring the dependence of the structure function $F_2(x,Q^2)$ on Q^2 at fixed Bjorken x ("scaling violations"). Such measurements can be done by observing just the scattered electron[1]. By studying in addition the hadronic final state, on the other hand, details of the parton dynamics, both in the perturbative and non-perturbative regime can be unraveled, as will become clear in the course of this lecture.

* Presented at the School on QCD, Low x Physics, Saturation and Diffraction, Copanello, Calabria, Italy, July 1–14, 2007.

[1] Here and in the following the term "electron" is used for both lepton polarities.

The lecture is structured as follows: First, the single particle spectra of the hadronic final state from *ep* reactions will be discussed. Then we focus on jets (collimated bundles of hadrons), which trace the original partons participating in the DIS scattering process. We will show that the measured cross-sections are generally well described by the evolution of the (non-perturbative) parton distributions with Q^2, as formulated by Altarelli and Parisi ("DGLAP" evolution). However, certain kinematic regions for jet production will be identified, where an alternative dynamics ("BFKL") may be at work. Flavor tagging of the jets (charm and beauty) will then be discussed as well as data on prompt photons (together with jets). All these hadronic final states, with some kind of "parton identification" are called semi-inclusive. Finally we discuss some exclusive final states and present, as a warning, the story of the rise and fall of some exotic baryon resonances which, if they exist, are made out of five quarks ("pentaquarks").

1.1. Deep inelastic scattering

Quantum Chromodynamics (QCD) is expected to describe the strong interactions between quarks and gluons. At distances small compared to the nucleon radius, or equivalently large momentum transfer Q^2 where the strong coupling $\alpha_{\rm S}$ is small, perturbative QCD (pQCD) gives an adequate quantitative account of hadronic processes. The total cross-sections, however, are dominated by long range forces ("soft interactions"), where a satisfactory understanding of QCD still remains a challenge. This is also of importance for all transitions of partons to hadrons in the final state ("fragmentation process"). In addition, non-perturbative effects govern the DIS kinematics through the momentum distribution ("parton distribution functions", or "pdfs") of the initial partons, interacting with the electrons via photon or Z^0 exchange (see Fig. 1). The latter is important only at very large Q^2, *i.e.* around or beyond the mass of the Z^0. The division between the non-perturbative and the perturbative regimes is defined by the factorization scale, which should be sufficiently large ($\mathcal{O}$(few GeV^2)) to hope for a convergent perturbative expansion in the strong coupling constant $\alpha_{\rm S}$.

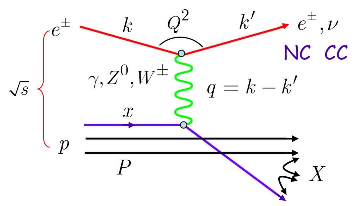

Fig. 1. Lowest order Feynman diagram for deep-inelastic electron–proton scattering in the parton picture, showing the relevant kinematical quantities characterizing inclusive DIS reactions (see text). The hadronic final state "fragmented" from the scattered and spectator partons is indicated by X.

1.2. Quantum chromodynamics in the HERA regime

Within the framework of perturbative QCD, the DIS cross-section at the parton level is generically given by

$$\sigma = \sum_i \sigma_{\gamma^* i}(Q^2) \otimes x f_i(x)\,, \tag{1}$$

where Q^2 is the virtuality of the exchanged boson (here: the virtual photon γ^*), x is the momentum fraction (Bjorken x) of the incoming parton, and $\sigma_{\gamma^* i}$ is the total virtual photon–parton cross-section. In this expression the factorization theorem of QCD [3] has been used, separating the cross-section into a hard scattering part between the exchanged virtual photon and the incoming parton i, convoluted with a non-perturbative part describing the momentum distribution $x f_i(x)$ of parton i within the proton. In Eq. (1) one recognizes the incoherent summing of quark contributions, which is justified by the property of asymptotic freedom. Asymptotic freedom states that the interaction between the partons within the proton, characterized by the strong coupling constant $\alpha_{\rm S}$, become weak at large Q^2 ($\alpha_{\rm S} \to 0$ as $Q^2 \to \infty$). In this way the scattering process of the electron with the partons of the proton can be treated incoherently.

Fig. 1 also indicates the kinematics in the HERA regime. Here, s is the square of the total ep center of mass energy. The four-momentum transfer squared Q^2 is given by the scattered electron alone, the Bjorken variable x and the inelasticity y (equal to the energy fraction transferred from the electron to the virtual photon in the proton rest frame) are given by

$$Q^2 = -(k-k')^2 = -q^2\,, \qquad x = \frac{Q^2}{2\,P\cdot q}\,, \qquad y = \frac{P\cdot q}{P\cdot k}\,. \tag{2}$$

Only two of the three quantities in Eq. (2) are independent, they are related via $Q^2 = sxy$. Another interesting quantity is the total mass M_X of the hadronic final state, given by

$$M_X^2 \equiv W^2 = (q+P)^2 = \frac{Q^2(1-x)}{x}\,. \tag{3}$$

This relation shows that low x reactions correspond, at fixed Q^2, to large values of W^2, *i.e.* large invariant masses of the hadronic final state. Due to the high colliding beam energies (protons at 920 GeV, electrons at 27.6 GeV), HERA provided a large range of exploration for x and Q^2, extending the reach of previous fixed target experiments by more than 2 orders of magnitude in x and Q^2.

The double differential cross-section for ep scattering is written as (see, *e.g.* [4])

$$\frac{d^2\sigma\,(e^{\pm}p)}{dx\,dQ^2} = \frac{2\pi\alpha^2}{xQ^4} Y_+ \left[F_2 - \frac{y^2}{Y_+} F_L \mp \frac{Y_-}{Y_+} xF_3 \right] , \tag{4}$$

where the functions $Y_\pm$ are given by $Y_\pm = 1 \pm (1-y)^2$, and the structure functions, apart from coupling constants, are combinations of the parton distribution functions. For the case of pure photon exchange, valid at low Q^2, one obtains

$$F_2(x) = \sum_{i=u,d,...} e_i^2 x f_i(x) \,, \tag{5}$$

where the sum extends over all partons of charge e_i within the proton. As indicated in Fig. 1, all reactions with neutral boson exchange are called "neutral current (NC)" reactions, those with $W^{\pm}$ exchange (here the final state lepton is a neutrino) are called "charged current (CC)" reactions.

The non-perturbative parton distribution functions $f_i(x)$ cannot be calculated from first principles and have therefore to be parameterized at some starting scale Q_0^2. Perturbative QCD predicts the variation of f_i with Q^2, *i.e.* $f_i = f_i(x, Q^2)$ via a set of integro-differential evolution equations, as formulated by Altarelli and Parisi ("DGLAP" equations, see [5]). The predicted Q^2 dependence ("scaling violations") of the structure function F_2, see Eq. (5), are nicely supported by the data from HERA [6].

2. General properties of the hadronic final state in *ep* collisions

If the hadronic final state is to be considered, one needs an additional step from the parton level discussed so far to the hadron level ("hadronization process"). This process is non-perturbative and one has to resort again to models describing this step. Similar to the parton distribution functions $f_i(x)$ one defines "fragmentation functions" $D_i(x_P)$, giving the probability that a final state hadron carries a certain momentum fraction x_P of the original parton i. Such functions can be experimentally determined from studies of single particle spectra. Also here a scale is necessary to separate, similar to the cross-section formula in Eq. (1), the fragmentation from the perturbative hard collision. This scale is naturally called "fragmentation scale" and can be chosen in the same way as the former.

The experimental investigations on the hadronic final state are preferentially carried out in the so-called Breit frame, which is defined as the frame where the virtual photon direction is collinear with the incoming charged parton, and where the parton momentum p^{Breit} is related to the photon momentum Q by $p^{\mathrm{Breit}} = Q/2$. In this frame the incoming parton absorbs the photon of momentum $-Q$ and is emitted into the reverse direction with momentum $-Q/2$. For this reason the Breit frame is sometimes also called the "brick wall frame".

2.1. Charged particle spectra

In the Breit frame two hemispheres can be defined: one in direction of the recoiling parton, which called the "current region", and the one into which the "proton remainder", *i.e.* the spectator di-quark system, is emitted. In the current region a single parton fragments into observable hadrons. If this fragmentation process is universal, *i.e.* does not depend on the way the initial partons are generated, the data from e^+e^- reactions should look very similar. In the latter case the hemispheres are divided by a plane spanned by the momentum vector of one of the final state quarks (event thrust axis).

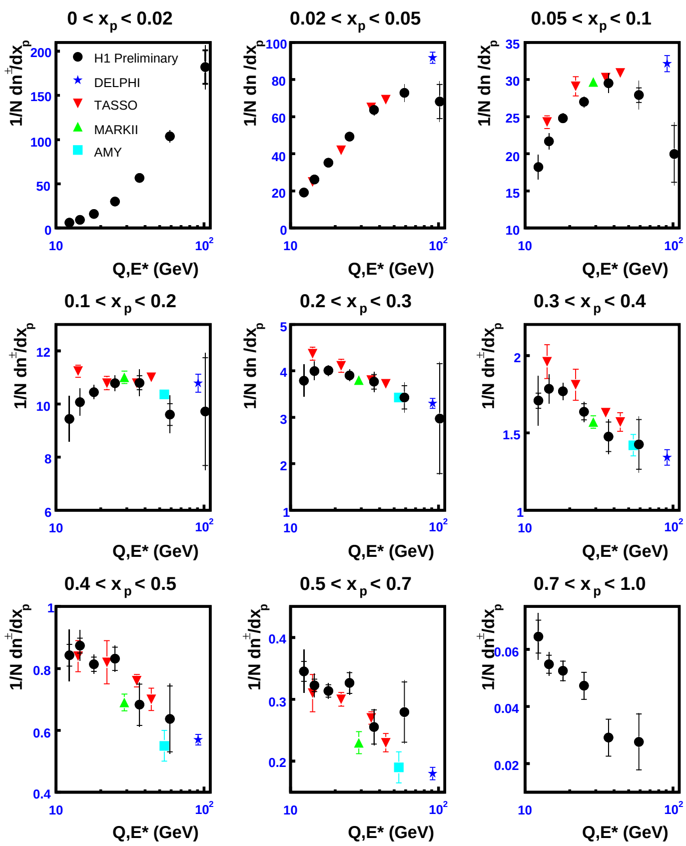

Fig. 2. Event-normalized scaled momentum distributions as functions of Q for different x regions from H1 [7]. Also shown are data from e^+e^- experiments, taking $Q = E^*$ (see text).

For comparison of the results from ep scattering and e^+e^- it is useful to consider the scaled momentum distribution of particles, where the scaled momentum x_p is given by $x_p = 2p^{\mathrm{Breit}}/Q$. Fig. 2 shows measurements [7] of x_p for charged particles from the H1 experiment for various values of Bjorken x as functions of Q. Similar measurements also exist from the ZEUS Collaboration [8]. The e^+e^- data are shown as well. Here, the particle momenta are rescaled to $x_p = p/E^*$, where $2E^* = \sqrt{s}$ is the e^+e^- center of mass energy. The HERA data in the current hemisphere generally agree with the e^+e^- data, supporting quark fragmentation universality. There are, however, some kinematic regions at lower vales of Q, where differences are indeed expected due to higher order QCD processes, such as boson–gluon fusion or QCD Compton scattering which cannot occur in e^+e^- reactions. Also, in the highest Q bin, but at low x, there is an excess in the e^+e^- data for which no evident reason exists.

In the representation of the data in Fig. 2 clear scaling violations (Q^2-dependences) are visible. Such effects can in principle be accommodated by higher order QCD calculations plus fragmentation of partons to hadrons according to some model. Various models have been tried by H1 and ZEUS (neither of them shown in the figure) and, generally, the string model of hadronization [9] gives better agreement than cluster models [10].

2.2. Strange particle production

An important test for the fragmentation models is the yield of strange particles, such as K^0_S, Λ and $\bar{\Lambda}$. Fig. 3 shows the data for K^0_S and $\Lambda, \bar{\Lambda}$ production from the ZEUS Collaboration [11] as functions of the transverse momentum and rapidity (similar data have been presented by the H1 Collaboration [12] recently). Neutral strange hadrons can be identified through their displaced decay vertex and a mass fit to the observed secondaries. The charged strange particles, such as $K^\pm$, are very difficult to separate from the other charged hadrons. A significant parameter which is governing the production of strange hadrons is the strangeness suppression factor λ_{s}. It describes the probability to produce s-quark pairs relative to u- and d-quark pairs in the string fragmentation. This parameter was determined from e^+e^- data to be $\lambda_{\mathrm{s}} = 0.3$. As can be seen from Fig. 3, the ARIADNE color dipole model (CDM) [13], implementing the Lund string fragmentation for the transition to the hadron level with the standard value for λ_{s} gives the best description of the data. There is no indication for any unusual yield of strange hadrons, as would be expected if QCD instanton effects [14] were making a significant contribution.

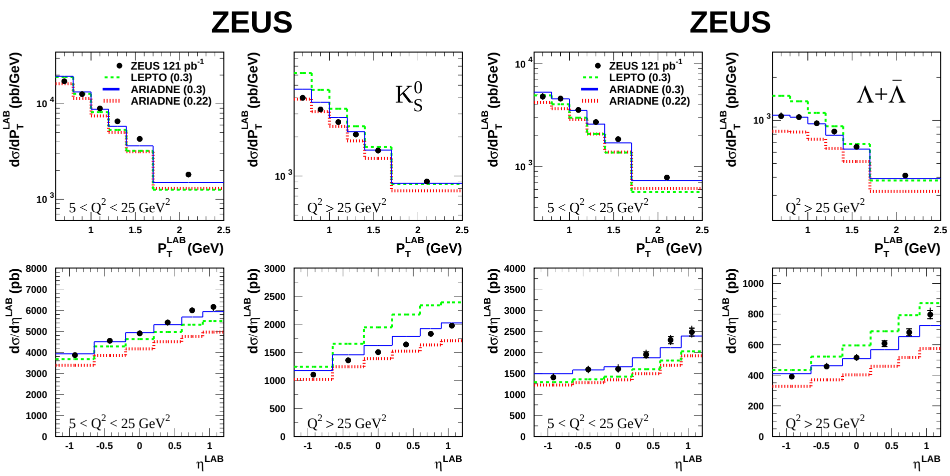

Fig. 3. Differential cross-sections for strange hadron production from the ZEUS experiment [11] as functions of $p_{\mathrm{T}}^{\mathrm{lab}}$ and η^{lab}. The variable η^{lab} is the rapidity in the lab system, defined by $\eta = -\ln\tan(\theta/2)$, where θ is the particle's polar angle. The histograms show predictions from ARIADNE and LEPTO using the stated strangeness suppression factors (see text).

3. Jets at HERA

Collimated bundles of particles ("jets") are believed to carry the kinematic information of the partons emerging from DIS reactions at HERA and other colliding beam experiments. The study of jet production is therefore a sensitive tool to test the predictions of perturbative QCD and to determine the strong coupling constant α_{S} over a wide range of Q^2.

Several algorithms exist to cluster individual final state hadrons into jets, but most commonly used at HERA is the so-called k_{T} clustering algorithm [15]. The jet finding is usually executed in the hadronic center of mass system. which is, up to a Lorentz boost, equivalent to the Breit frame. At the end of the algorithm, the hadrons are collected into a number of jets.

At leading order (LO) in α_{S}, di-jet production (see Fig. 4) proceeds via the QCD Compton process ($\gamma^* q \to qg$) and boson–gluon fusion ($\gamma^* g \to q\bar{q}$). The cross-section for events with three jets is of $\mathcal{O}(\alpha_{\mathrm{S}}^2)$. These events can be interpreted as coming from a di-jet process with additional gluon radiation or gluon splitting (see caption of Fig. 4), bringing the QCD calculation to next-to-leading order (NLO).

In jet physics, two different "hard" scales can be used to enable NLO (and higher) calculations: the variable Q, and the transverse energy E_{T} of the jets. Fig. 5 shows the differential cross-sections for inclusive jet production at high Q^2 as measured by the ZEUS Collaboration [16], both with respect

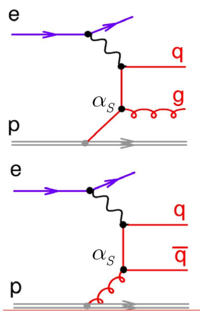

Fig. 4. Feynman diagrams for LO jet production. The upper subgraph is called "QCD Compton", the lower subgraph is called "boson–gluon fusion". Both graphs contribute to two-jet final states. Events with three jets can be interpreted as a di-jet process with additional gluon radiation from one of the involved quark lines, or as a gluon splitting into a quark–antiquark pair. These processes are of the order of $\mathcal{O}(\alpha_{\rm S}^2)$ (NLO).

to Q^2 and $E_{\rm T}$. The data are compared to NLO calculations, using the renormalization and factorization scales as indicated in the figure. Both schemes are able to describe the data very well, indicating the validity of the choice of any of the two hard scales. Given the experimental and theoretical uncertainties at these large scales, no higher order (beyond NLO) corrections seem necessary.

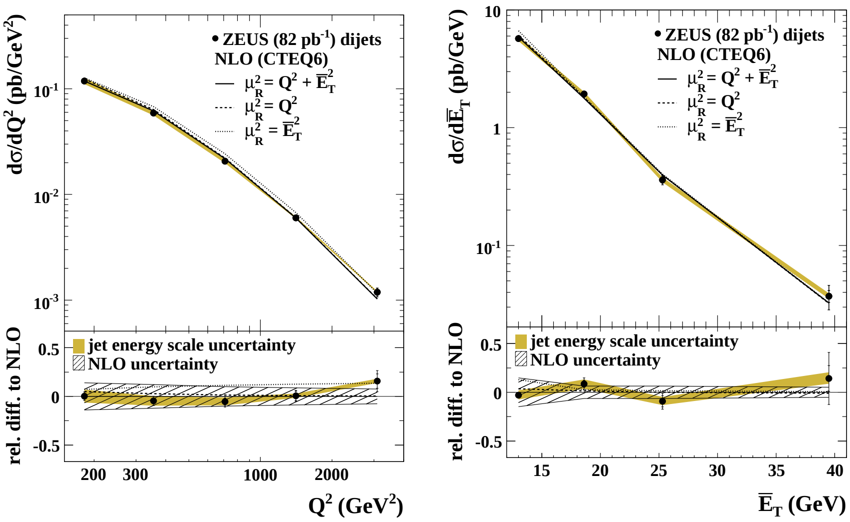

Fig. 5. Differential cross-sections for inclusive jet production from the ZEUS experiment [16]. Also shown are the predictions from next-to-leading order QCD calculations, which give a good description of the data.

3.1. The strong coupling constant

One of the most important measurements using multi-jet final states is the determination of the strong coupling constant α_{S}. At HERA, this measurement is particularly interesting, since α_{S} can be determined in a single experiment over a large range of Q or E_{T}. Observables which are sensitive to α_{S} come from various sources, such as inclusive jets, jet ratios (number of three jets relative to the number of two jets), and event shape variables (thrust, jet masses, angles between jets *etc.*). A recent compilation of α_{S} determinations [17] from the two HERA experiments H1 and ZEUS, using various jet observables, is shown in Fig. 6. An NLO fit to these data yields a combined value of $\alpha_{\mathrm{S}}(M_Z) = 0.1198 \pm 0.0019(\mathrm{exp.}) \pm 0.0026(\mathrm{th.})$. The dominating theoretical error arises from the uncertainty due to terms beyond NLO, which is estimated by varying the renormalization scale by the "canonical" factors 0.5 and 2.

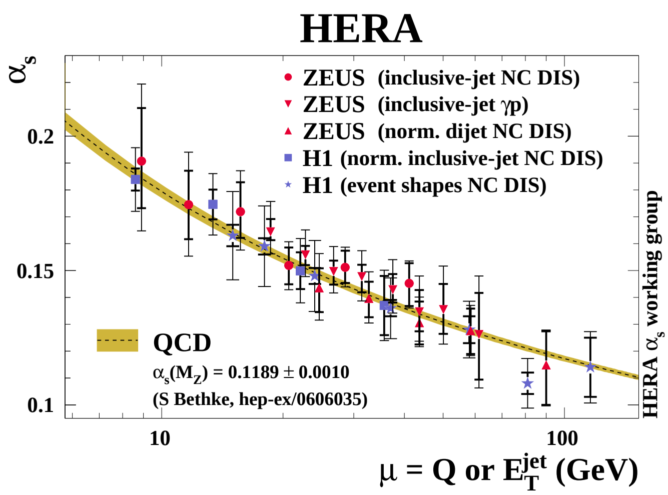

Fig. 6. Compilation of $\alpha_{\mathrm{S}}(\mu)$ measurements from H1 and ZEUS [17], based on jet variables as indicated. The dashed line shows the two loop solution of the renormalization group equation, evolving the 2006 world average for $\alpha_{\mathrm{S}}(M_Z)$. The band denotes the total uncertainty of the prediction.

3.2. Forward jets

All of the analyses regarding the observables mentioned in the previous chapters rest on the DGLAP Q^2 evolution scheme for the pdfs involved. Potential deviations observed a certain regions of phase space (low x, low Q^2) are usually attributed to the limited order of the presently computed QCD matrix elements (LO, NLO, sometimes NNLO). Especially for low x ($\approx 10^{-4}$), but sufficiently large Q^2 ($>$ a few GeV^2), there has been a vivid debate about the validity of the DGLAP approach. In this kinematic regime the initial parton in the proton can induce a QCD cascade, consisting of several subsequent parton emissions, before eventually an interaction with the virtual photon takes place (see Fig. 7). QCD calculations based on the "direct" interaction between a point-like photon and a parton from the evolution chain, as given by the DGLAP approach, are very successful in describing, *e.g.* the unexpected rise of F_2 with decreasing x over a large range in Q^2 [18].

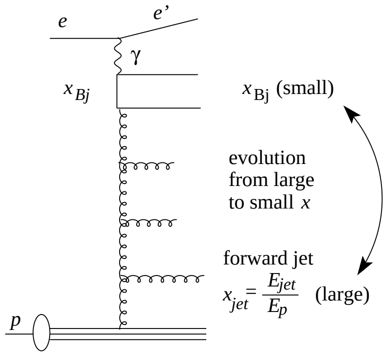

Fig. 7. Schematic diagram of ep scattering producing a forward jet. The evolution in the longitudinal momentum fraction x, from large x_{jet} to small x_{Bj}, is indicated.

For low values of x, there is, however, a technical reason to question the validity of the DGLAP evolution approach: Since it resums only leading $\log(Q^2)$ terms, the approximation may become inadequate for very small x, where $\log(1/x)$ terms become important in the evolution equations. In this region the BFKL scheme [19] is expected to describe the data better, since in this scheme terms in $\log(1/x)$ are resummed.

The large phase space available at low x (see Eq. (3)) makes the production of forward jets (in the angular region close to the proton direction) a particularly interesting topic for the study of parton dynamics, since jets emitted in this region lie well away in rapidity from the photon end of the evolution ladder (see Fig. 7). Concerning the forward jets there is a clear dynamic distinction between the DGLAP and BFKL schemes: In the DGLAP scheme, the parton cascade resulting from hard scattering of the virtual photon with a parton from the proton is ordered in parton virtuality. This ordering along the parton ladder implies an ordering in transverse energy E_{T} of the partons, so that the parton participating in the hard scatter has the highest E_{T}. In the BFKL scheme there is no strict ordering in virtuality or transverse energy. The BFKL evolution therefore predicts that a larger fraction of low x events will contain high-E_{T} forward jets than is predicted by the DGLAP evolution.

Both ZEUS [21] and H1 [20] have studied forward jet production, where "forward" typically means polar emission angles less than about 20 degrees relative to the proton direction. As a first example, the single differential cross-sections $d\sigma/dx$ from H1 are shown in Fig. 8. The data are compared to LO and NLO QCD calculations [22] (a), and several Monte Carlo models ((b) and (c)). The NLO calculation in (a) is significantly larger than the LO calculation. This reflects the fact that the contribution from forward jets in the LO scenario is kinematically suppressed. Although the NLO contribution opens up the phase space for forward jets and considerably improves the description of the data, it still fails by a factor of 2 at low x. In Fig. 8(b) the predictions from the CASCADE Monte Carlo program [23] is shown, which is based on the CCFM formalism [24]. The CCFM equations provide a bridge between the DGLAP and BFKL descriptions by resumming both $\log(Q^2)$ and $\log(1/x)$ terms, and are expected to be valid over a wider x range. The model predicts a somewhat harder x spectrum, and fails to describe the data at very low x. In part (c) of the figure, the predictions ("RG-DIR") from the LO Monte Carlo program RAPGAP [25] is shown, which is supplemented with initial and final state parton showers generated according to the DGLAP evolution scheme. This model, which implements only direct photon interactions, gives results similar to the NLO calculations from part (a), and falls below the data, particularly at low x. The description is significantly improved, if contributions from resolved virtual photon interactions are included ("RG-DIR+RES"). However, there is still a discrepancy in the lowest x bin, where a possible BFKL signal would be expected to show up most prominently. The Color Dipole Model (CDM) [13], which allows for emissions non-ordered in transverse momentum, shows a behavior similar to RG-DIR+RES.

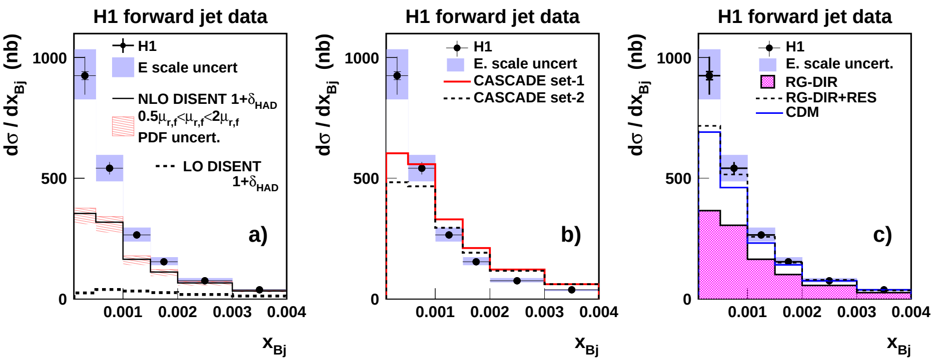

Fig. 8. Single differential cross-sections for forward jets as functions of x from the H1 experiment [20], compared to NLO predictions [22] in (a), and QCD Monte Carlo models [13, 25] in (b) and (c). The dashed line in (a) shows the LO contribution.

For a more detailed study the forward jet sample was divided into bins of $p^2_{\rm t,\,jet}$ and Q^2. The triple differential cross-section $d^3\sigma/dxdQ^2dp^2_{\rm t,\,jet}$ *versus* x is shown in Fig. 9 for several regions in Q^2 and $p^2_{\rm t,\,jet}$. In addition, the expectations from the above mentioned QCD models are presented. Using the ratio $r = p^2_{\rm t,\,jet}/Q^2$, various regimes can be distinguished: For $p^2_{\rm t,\,jet} < Q^2$ ($r < 1$) one expects a DGLAP-like behavior, dominated by direct photon interactions (see Fig. 9 (c)). Due to the large bin sizes, however, the ranges of r can be quite large, so that r in this bin can assume values up to 1.8 due to admixtures from events with $p^2_{\rm t,\,jet} > Q^2$. This may explain why the DGLAP direct model (RG-DIR), although closer to the data in this bin than in any other, does not quite give agreement with the data except at the highest x-bin. In the region $p^2_{\rm t,\,jet} \approx Q^2$ ($r \approx 1$, see Fig. 9 (b) and (f)),

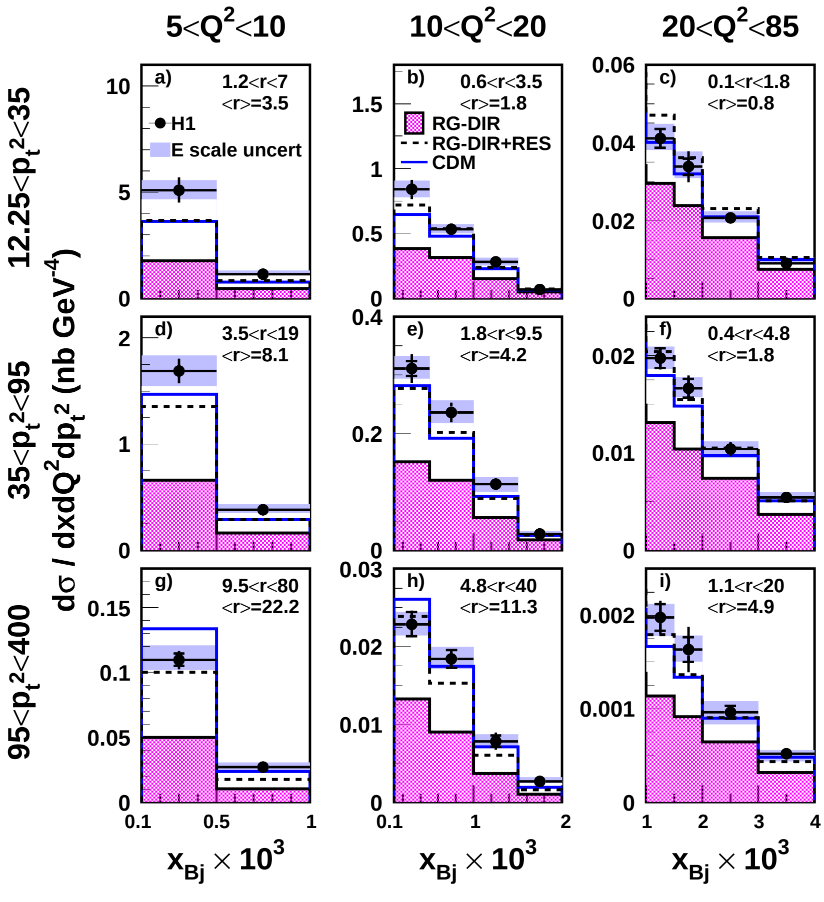

Fig. 9. Triple differential cross-sections for forward jet production as function of x in bins of Q^2 and $p^2_{\rm t,\,jet}$, compared to various Monte Carlo calculations (see text).

DGLAP suppresses parton emission, so that BFKL dynamics may show up. However, the DGLAP resolved model (RG-DIR+RES) describes the data reasonably well.

The regime of $p^2_{\mathrm{t,\,jet}} > Q^2$ ($r > 1$, see Fig. 9 (d), (g) and (h)), is typical for processes where the virtual photon is resolved, *i.e.* the incoming parton from the proton vertex interacts with a parton from the photon. As expected, the DGLAP resolved model (RG-DIR+RES) provides a good overall description of the data, again similar to the CDM model. However, it can be noted that in regions where r is largest and x is small, CDM shows a tendency to overshoot the data. DGLAP direct (RG-DIR), on the other hand, gives cross-sections which are too low. Although the above analysis tries to isolate "BFKL regions" from "DGLAP regions", the conclusion on underlying dynamics cannot be reached, most importantly since the "BFKL region" ($r \approx 1$) is apparently heavily contaminated by "DGLAP-type" events. In addition, the two "different" evolution approaches, RG-DIR+RES ("DGLAP") and CDM ("BFKL"), give similar predictions.

In a further step, the parton radiation ladder (see Fig. 7) is examined in more detail by looking also at jets in the region of pseudorapidity, $\eta = -\ln\tan(\theta/2)$, between the scattered electron (η_e) and the forward jet (η_{forw}). In this region a "2-jet + forward" sample was selected, requiring at least 2 additional jets, with $p_{\mathrm{t,\,jet}} > 6$ GeV for all three jets, including the forward jet. In this scenario, evolution with strong k_{t} ordering is obviously disfavored. The jets are ordered in rapidity according to $\eta_{\mathrm{forw}} > \eta_{\mathrm{jet2}} > \eta_{\mathrm{jet1}} > \eta_e$. Two rapidity intervals are defined between the two additional jets and the forward jet (see Fig. 11): $\Delta\eta_1 = \eta_{\mathrm{jet2}} - \eta_{\mathrm{jet1}}$ is the

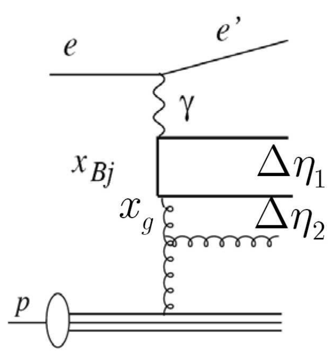

Fig. 10. Kinematic regions for the event sample "2-jets + forward" (see text). The quarks in the photon–gluon fusion process are q_1 (upper solid line) and q_2 (lower solid line). The rapidity gap between q_1 and q_2 is denoted by $\Delta\eta_1$, the gap between q_2 and the forward jet is denoted by $\Delta\eta_2$.

rapidity interval between the two additional jets, and $\Delta\eta_2 = \eta_{\rm forw} - \eta_{\rm jet2}$ is the interval between jet 2 and the forward jet. If the di-jet system originates from the quark line coupling to the photon (see Fig. 11), the phase space for evolution in x between the di-jet system and the forward jet is increased by requiring that $\Delta\eta_1$ is small and that $\Delta\eta_2$ is large: Requiring $\Delta\eta_1 < 1$ will favor small invariant masses of the di-jet system. As a consequence, x_g will be small, leaving the rest for additional radiation. When, on the other hand, $\Delta\eta_1$ is required to be large ($\Delta\eta_1 > 1$) BFKL-like evolution may then occur between the two jets from the di-jet system or, when both $\Delta\eta_1$ and $\Delta\eta_2$ are small, between the di-jet system and the hard scattering vertex. Note that the rapidity phase space is restricted only for the forward jet.

As argued above, this study disfavors evolution with strong ordering in $k_{\rm t}$ due to the common requirement of large $p_{\rm t,\,jet}$ for the three jets. Radiation which is not ordered in $k_{\rm t}$ may occur at any location along the evolution chain, depending on the values of $\Delta\eta_1$ and $\Delta\eta_2$. Fig. 11 show the measured cross-sections as function of $\Delta\eta_2$ for all data, and separated into the two regions of $\Delta\eta_1$ discussed above. One can see that here the CDM model is in a good agreement with the data in all cases, while the DGLAP models predict cross-sections which are too low, except when both $\Delta\eta_1$ and $\Delta\eta_2$ are large. For this topology all models (and the NLO calculation, not shown) agree with the data, indicating that the available phase space for evolution is exhausted.

It is important to realize that the "2+forward jet" sample indeed seems to differentiate between the CDM and DGLAP resolved models, in contrast to the more inclusive samples (see Fig. 9). The conclusion is that additional

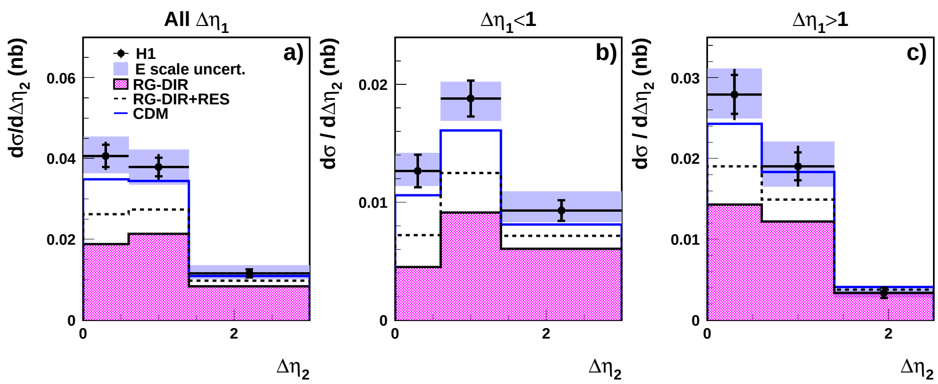

Fig. 11. Cross-section for events with a reconstructed high transverse momentum di-jet system and a forward jet from the H1 experiment [20], as function of $\Delta\eta_2$ for two regions of $\Delta\eta_1$. The data are compared to predictions of "DGLAP-like (RG-DIR+RES) and "BFKL-like" (CDM) Monte Carlo models (see text).

breaking of the $k_{\rm t}$ ordering, beyond what is included in the resolved photon model, is required by the data, pointing towards some evidence for BFKL dynamics. It is, however, not excluded that such effects may also be described by higher order DGLAP calculations, which may become available in the future.

4. Open charm and beauty production

Low x physics processes at HERA are dominated by gluonic contributions and are therefore governed by the gluon distribution function within the proton. This function can be determined indirectly from the scaling violations of the structure function F_2, as measured in DIS inclusive ep scattering (see, *e.g.*, [26] for recent results on pdfs from a QCD fit to the combined data of H1 and ZEUS). A more direct way to access the gluon distribution is to select boson–gluon fusion processes (see Fig. 4, lower graph). In order to suppress the QCD Compton part (Fig. 4, upper graph), the quark loop should contain heavy quarks not present in the proton, *i.e.* charm or bottom quarks. The production of c and b quarks in ep collisions also provides stringent tests for perturbative QCD, since the heavy quark masses ($m_c^2 \approx 10$ GeV^2, $m_b^2 \approx 25\,$GeV^2) can serve as hard scales to ensure reliable perturbative calculations.

Heavy quarks in the final state are identified by various methods: c quarks are usually identified by explicit reconstruction of a D^* meson. Such methods, however, drastically reduce the statistics due to the small branching ratios into particular final states. For b quarks, explicit reconstruction at HERA is impossible due to lack of statistics in any of the very many exclusive final states. Production of hadrons with b quarks, however, can be enhanced by requiring the presence of one or more jets, tagged by a muon or electron from the semileptonic decay of one of the b quarks.

There is an alternative method to tag heavy quark production: With the help of high-precision micro-vertex detectors, mesons containing heavy quarks are distinguished from those containing only light quarks by reconstructing the displacement of the decay tracks from the primary vertex, caused by the short (but finite) lifetime of these mesons. The clear advantage of this method is that all decay channels of the charm/bottom hadrons can be used and the phase space for heavy quark selection need not be restricted. A problem, however, is to separate charm from bottom, in particular at low Q^2, since the b production at HERA is expected to be small compared to charm.

Fig. 12 shows the data from H1 [27] and ZEUS [28] on the structure functions F_2^{cc} and F_2^{bb}, which are derived from the reduced cross-section, dividing out the kinematic terms divided given in Eq. (4), according to

$$\tilde{\sigma}_{c\bar{c},b\bar{b}} \equiv \frac{d^2\sigma^{c\bar{c},b\bar{b}}}{dxdQ^2}\left(\frac{xQ^4}{2\pi\alpha(1+(1-y)^2)}\right) = F_2^{c\bar{c},b\bar{b}} - \frac{y^2}{1+(1-y)^2}F_{\mathrm{L}}^{c\bar{c},b\bar{b}}\,. \quad (6)$$

Here, the small contribution from the longitudinal structure function $F_{\mathrm{L}}^{c\bar{c},b\bar{b}}$ is estimated from NLO QCD predictions [29, 30], based on the variable flavor number scheme (VFNS), to be discussed subsequently. Also shown are previous measurements for F_2^{cc} from H1 [31] and ZEUS [32] based on D^* tagging. Due to the limited acceptance for clean reconstruction of D^*'s in the final state, the data need to be extrapolated to the full solid angle, which has been done by using an NLO program [33] for charmed quark pair production, based on DGLAP evolution.

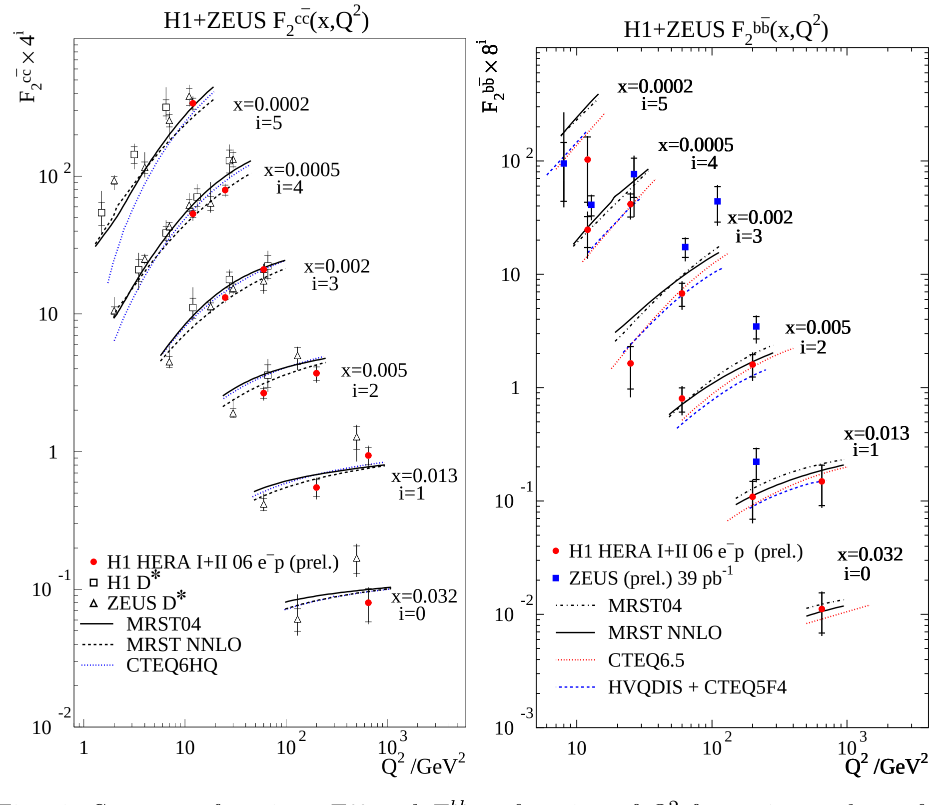

Fig. 12. Structure functions F_2^{cc} and F_2^{bb} as function of Q^2 for various values of x from HERA (see text). The QCD predictions differ mainly by their pdfs.

The data from the two experiments are in reasonable agreement and also agree with the previous measurements using D^* tagging. There is a tendency, however, for the ZEUS data to lie above the H1 data, both for charm and bottom production. Comparisons are made with the above mentioned NLO QCD predictions, which are able to describe the data. The precision of the data is not yet sufficient to distinguish between the predictions, which are based on 4 different pdfs.

For the comparison of QCD with the measurements of the structure function $F_2^{c\bar{c},b\bar{b}}$ one has to choose DIS events to have a hard scale, here Q^2. For b quark production, however, DIS is plagued with very low cross-sections, so that stringent tests of QCD models is hampered by low statistics. A way to substantially increase the statistics is to go down in Q^2 (photoproduction) and select a different hard scale for the comparison with perturbative QCD calculations. Such a scale can be provided by considering jet production with b-quarks (hard scale is E_{T} of the jet), or even forget about the jet selection to increase the statistics even more, and use the mass of the b-quark itself as the hard scale. An interesting analysis of the latter type has been presented by the ZEUS collaboration [34], looking into events with two muons, without any requirement on jets or p_t of the muons.

The principle of selecting an almost background-free sample with b-quark production is to look for like-sign di-muon events. Like-sign di-muons can only originate from the decays of different b-quarks, where one μ is from a semileptonic b-quark decay, and the other μ is from the semileptonic $\bar{c}$ decay (after a hadronic decay of the $\bar{B}$-hadron in an anti-charmed meson). Unlike-sign muons come from the same parent B-hadron, *e.g.* through the decay chain $b \to c\mu X \to s\mu\mu X'$, or from the semileptonic decays of the B- and $\bar{B}$-hadrons. Beauty production is the only source of genuine like-sign muons, backgrounds from light flavors are well controlled, contributing equally to like-sign and unlike-sign di-muon events.

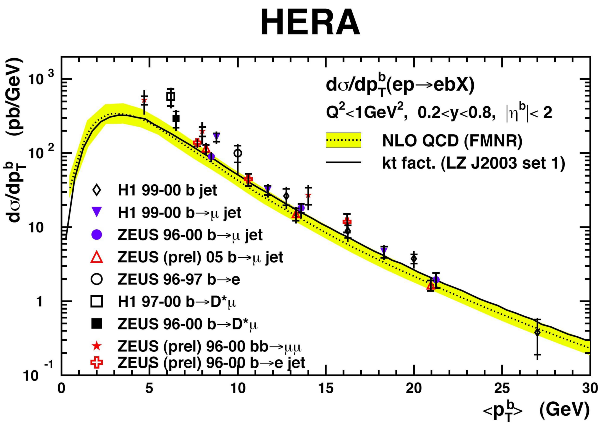

Fig. 13. Measured differential cross-sections for b-quark production as function of p_{t} of the b-quark, summarizing all photoproduction data from HERA [35]. Also shown is the corresponding NLO expectation (see text).

Fig. 13 shows a recent compilation of the differential cross-section for b-quark photoproduction for all HERA data [35] together with the NLO expectation [36]. In contrast to DIS c-quark production, where the theory is in agreement with the measurement (not shown here), the prediction for b-quark photoproduction is lower by about a factor of 2 over most of the p_{t} range. As can be seen, the data from H1 [37] agree with the ZEUS data. A similar factor, in mutual agreement, has also been found in deep-inelastic production of b-quarks by H1 [38] and ZEUS [39].

5. Prompt photons

Photons originating from partonic interactions provide a sensitive probe for precision tests of perturbative QCD and yield information on the structure of the proton, when they are radiated from the quark lines. Such photons, coupling to the interacting partons, are often called "prompt", as opposed to photons from hadron decays or photons radiated by leptons. In contrast to measurements using hadrons, prompt (or isolated) photons minimize uncertainties from parton fragmentation, hadronization or jet identification. Furthermore, the experimental uncertainties of the energy measurement are smaller for electromagnetic showers initiated by photons than for hadronic showers initiated by jets. On the other hand, there is a substantial background coming from π^0 decays, which outnumber the prompt photons by a large factor.

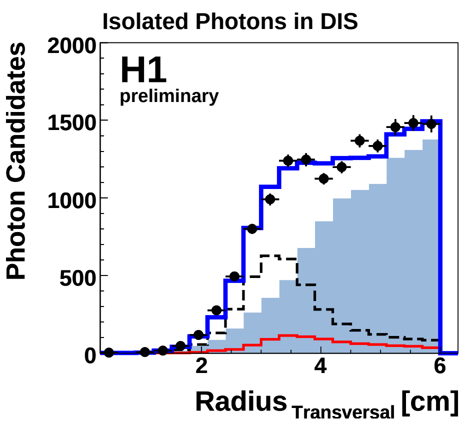

Fig. 14. Distribution of the transverse cluster radius for photon candidates from the H1 analysis [40]. Also shown are the contributions from π^0 decay (shaded histogram), the photons radiated off the lepton line (thin solid histogram, and the contribution from the "prompt" photons, radiated off the quark line (dashed histogram).

The isolated photon signal can be extracted in several ways. The one used by H1 [40] exploits the fine granularity LAr calorimeter information in order to determine a number of "shower shape variables" from the isolated electromagnetic clusters associated with photon candidates. ZEUS [41] uses its presampler in front of the barrel electromagnetic calorimeter to convert the photons to e^+e^- pairs. For the case of H1, Fig. 14 shows one of six shower shape variables, which characterizes the transverse size of the photon shower. The data are compared to the expectation from various sources, using the properly adjusted Monte Carlo simulations RAPGAP [25] for the photons from the electron line ("LL", thin solid histogram), and PYTHIA [42] for the prompt photons from the quark line ("QQ", dashed histogram). The π^0 background is simulated in both LO programs at the end of a parton shower step with subsequent Lund string fragmentation into final state hadrons (shaded histogram). The thick solid histogram, well describing the data, is the sum of all contributions.

Fig. 15 shows the differential cross-section for isolated photon production as function of the photon rapidity η^γ and Q^2 at the electron vertex. The data are compared with a LO ($\mathcal{O}(\alpha^3)$) calculation [43], where the individual contributions from the lepton line, the quark line and the sum, including the interference term, are shown. The prediction underestimates the data by almost a factor of 2, clearly indicating the need for higher order corrections in the pQCD calculation. The prediction comes closer to the data, when in addition to the prompt photon a jet is required.

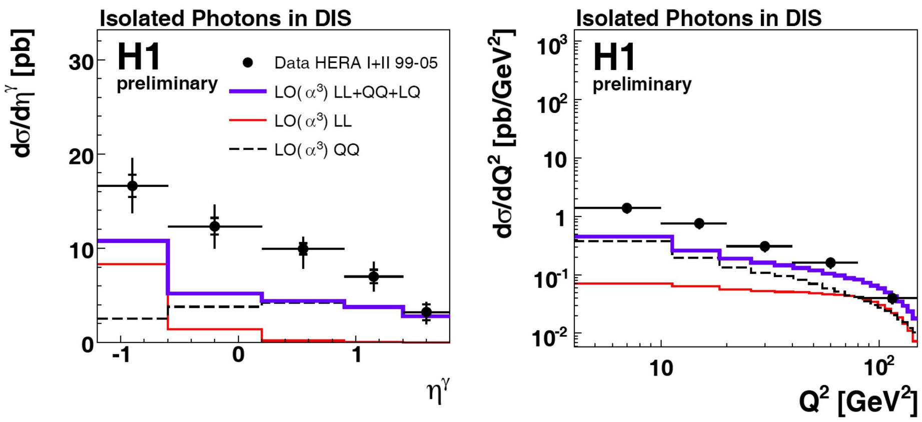

Fig. 15. Differential cross-section for the production of isolated photons as functions of η^γ and Q^2. The NLO calculations [43] are also shown (see text).

6. Specific final states

All the differential cross-sections for inclusive or semi-inclusive hadronic final states in *ep* reactions discussed so far were characterized by a hard scattering (short distance) process at the parton level, which provided the basis for their theoretical description within the framework of perturbative QCD. The total cross-section, on the other hand, is dominated by soft interactions, characterized by an almost energy-independent cross-section. A large fraction of these soft interactions is mediated by color-singlet (vacuum quantum number) exchange, and is termed "*diffractive*". In hadronic interactions, diffraction is well described by Regge theory (see, *e.g.* [44] for a review). In Regge theory, diffractive processes are formulated as a t-channel exchange of a leading trajectory with vacuum quantum numbers, called the "Pomeron" trajectory. In the high energy limit, Pomeron exchange dominates over all other contributions to the scattering amplitude and thus represents an essential non-perturbative feature of strong interactions.

In contrast to DIS, diffractive reactions tend to produce low mass hadronic systems X (see Fig. 1) and, quite frequently, the proton stays intact ($M_X = M_p$). Elastic scattering is a particular example for such a diffractive process. Measurements at HERA of the total photoproduction cross-sections for the reactions $\gamma p \to \mathrm{VM}\ p$ (VM $= \rho, \omega$, and ϕ) as function of the photon–proton center-of-mass energy $W_{\gamma p}$ [45–48] have beautifully verified the expected universal Regge behavior.

The cross-section for elastic photoproduction of J/ψ mesons, $\gamma p \to J/\psi\, p$, on the other hand, was observed [49, 50] to rise steeply with $W_{\gamma p}$, incompatible with a universal Pomeron. Due to its large mass, providing a "hard" scale (equivalent to a short range of the forces involved), the elastic photoproduction of J/ψ mesons is expected to be described by pQCD. This is even more so in electroproduction, where the photon virtuality Q^2 can provide a second hard scale. The presence of two hard scales makes J/ψ production particularly interesting for comparisons with pQCD. For a discussion of the experimental and theoretical status of elastic J/ψ production at HERA see, *e.g.* [51].

6.1. Spectroscopy: the pentaquark saga

This last section, on spectroscopy, should serve as a warning to all experimenters searching for new (expected or unexpected) signals in hadronic (or other) final states. The story goes as follows: Starting in the year 2003, there has been quite some interest in a new class of hadronic states, triggered by the report for evidence [52] of a narrow exotic baryon resonance with strangeness $S = +1$, realizable only with a five-quark system ("pentaquark"), containing a strange anti-quark ($uudd\bar{s}$). The findings were promptly confirmed by two other experiments [53, 54], each of them reporting a significance exceeding 4 σ. Also the theoretical justification for the possible existence of an entire multiplet (in fact an anti-decuplet, see Fig. 16) of such states had been given earlier [55].

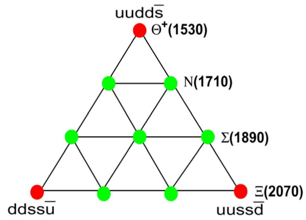

Fig. 16. Pentaquark anti-decuplet, as predicted by the model of Diakonov, Petrov and Polyakov [55]. They predicted the lightest state, Θ^+, to have a mass around 1530 MeV, with a width of about 15 MeV. The quark content of this state is $uudd\bar{s}$. The states below the Θ^+ increase in mass and strangeness content.

The so-called $\Theta^+(1530)$ resonance was reported in low energy fixed target experiments using photon or K^+ beams on nuclear targets. The signals were found in the invariant masses of the states nK^+ (*e.g.* by [54]) and $pK_{\rm S}$ (*e.g.* by [53]), the former carrying manifestly the strangeness quantum number $S = +1$, with a significance level of even 5.2 σ (see the signal from the CLAS Collaboration [54], Fig. 17). Within a few months following the announcements a total of 10 experiments (see [58] for a compilation), each with a significance in excess of 4σ (!) had confirmed the narrow signal

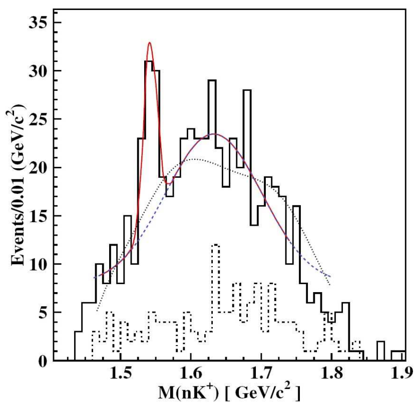

Fig. 17. Invariant mass spectrum of neutron and K^+ from the CLAS experiment [54] from the reaction $\gamma d \to K^+K^-p(n)$. The neutron 4-vector has been found by kinematic constraints. The exotic state with strangeness $S = +1$ has an intrinsic width of less than 21 MeV [54].

(measured widths less than about 10 MeV). Not enough with that, further anti-decuplet states where searched for and indeed found [57], such as the double strange states Ξ^{--} and Ξ^0 (see the anti-decuplet in Fig.16).

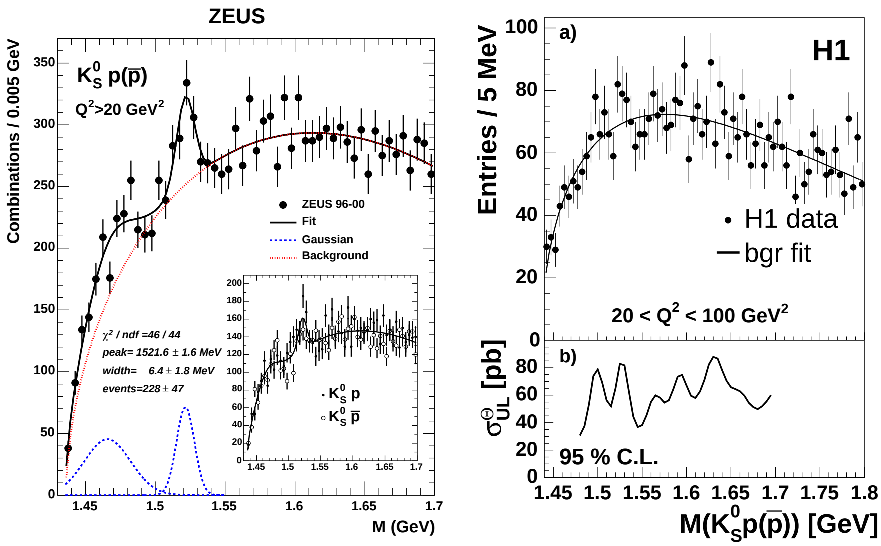

Fig. 18. Signal [59] and limits [60] for the strange pentaquark candidate $\Theta^+(1530)$.

Also at HERA the $\Theta^+(1530)$ was searched for. The ZEUS Collaboration reported confirmation, while H1 did not see a signal (see Fig. 18). However, H1 found evidence for yet another pentaquark by looking into the final state pD^{*-}, a narrow state around 3.1 GeV (see Fig. 19, left side). This state apparently contained a $\bar{c}$-quark, for sure a pentaquark state, if the signal were real. These data came from the running period until the year 2000, *i.e.* before the HERA luminosity upgrade. The analysis was later on repeated with the high statistics data after the upgrade and no signal was found ([62], see Fig. 19, right): The year 2000 data were a statistical fluctuation, albeit having produced a significance of 5.4 σ. In the subsequent years after 2003 many experiments have been carried out to search for the alleged pentaquark states, with the result that the evidence for any of theses states was fading away, in many cases via repetition of the experiment with high statistics, like in the H1 case. A recent report on the status of all these experiments can be found elsewhere [56], the pentaquark states may have exhausted their ephemeral life. The lecture to learn from this is to be very careful with signals with apparently large significance from small statistics, sometimes generated by cuts only motivated to enhance the fluctuation [58]. It will be interesting to follow the hoped-for future signal extractions at the Tevatron and at the LHC.

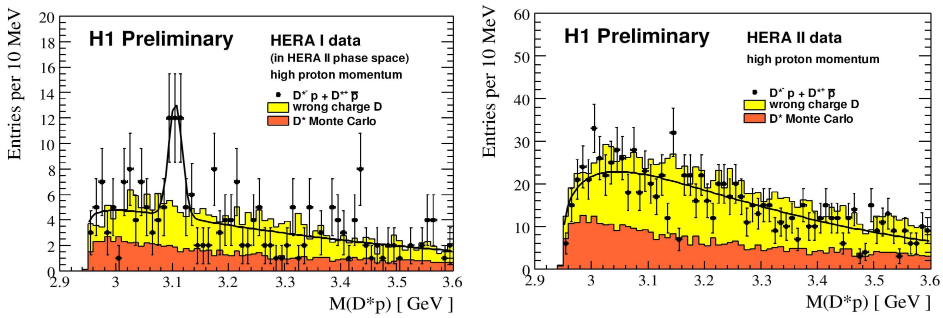

Fig. 19. Rise (HERA I data) and fall (HERA I and II data) of the charmed pentaquark in the H1 experiment [62].

7. Summary and conclusions

We have presented results on hadronic final states from deep inelastic ep collisions at low Bjorken x, observed at the HERA collider. The reason for studying details of the hadronic final state in DIS (and photoproduction) is to provide data for precise tests of perturbative QCD and to search for kinematic regions where concurrent QCD models can be distinguished. In most cases the DGLAP evolution scheme is describing the HERA data to an excellent degree. Among others, we presented the specific example of forward jets, where the need for new dynamics (BFKL) may be suggested.

There was also a warning given about the danger of producing signals which may be suspected to exist, sometimes through theoretical prejudice, and which demonstrates the importance of psychological factors in the analysis, especially when the statistics is low and the wish to find something new is strong.

The author is very much indebted to the organizers of the QCD Summer School in Calabria for the excellent preparation and smooth running of the meeting in an absolutely charming surrounding, as well as for the very warm and relaxed, but nevertheless highly stimulating, atmosphere they were able to create. He also acknowledges the careful reading of the manuscript and the helpful suggestions by his colleague Vladimir Chekelian.

REFERENCES

[1] H1 Collaboration, *Nucl. Instrum. Methods* **A386**, 310 (1997); **A386**, 348 (1997).

[2] ZEUS Collaboration, U. Holm ed., The ZEUS Detector, status report (unpublished), DESY (1993), available on
`http://www-zeus.desy.de/bluebook/bluebook.html`

[3] See, *e.g.*, J.C. Collins, D.E. Soper, *Annu. Rev. Nucl. Part. Sci.*, **37**, 383 (1987).

[4] F. Halzen, A.D. Martin, *Quarks and Leptons: An Introductory Course in Modern Particle Physics*, John Wiley & Sons, New York 1984.

[5] V.N. Gribov, L,N. Lipatov. *Sov. J. Nucl. Phys.* **15**, 438 (1972); G. Altarelli, G. Parisi. *Nucl. Phys.* **B126**, 298 (1977); Yu.L. Dokshitzer, *JETP* **46**, 641 (1977).

[6] H1 and ZEUS Collaborations, H1prelim 07-007, ZEUS-prel 07-026, DESY preprints 2007.

[7] H1 Collaboration, preprint DESY-07-065, 2007.

[8] ZEUS Collaboration, preprint ZEUS-prel-07-006, 2007.

[9] B. Andersson *et al., Phys. Rep.* **97**, 31 (1986).

[10] B.R. Webber, *Nucl. Phys.* **B238**, 492 (1984); C. Marchesini, B.R. Webber, *Nucl. Phys.* **B310**, 461 (1988).

[11] ZEUS Collaboration, DESY preprint DESY-06-226, Dec. 2006.

[12] H1 Collaboration, H1-prelim-08-034, Apr. 2008.

[13] L. Lönnblad, *Comput. Phys. Commun.* **71**, 15 (1992).

[14] See, *e.g.*, G. 't Hooft, *Phys. Rep.* **142**, 357 (1986); A. Ringwald *et al., Nucl. Phys.* **B365**, 3 (1991).

[15] S.D. Ellis, D.E. Soper, *Phys. Rev.* **D48**, 3160 (1993).

[16] ZEUS Collaboration, *Nucl. Phys.* **B765**, 1 (2007).

[17] H1 and ZEUS Collaborations, H1prelim-07-132, ZEUS-prel-07-025.

[18] H1 Collaboration, *Eur. Phys. J.* **C13**, 609 (2000); ZEUS Collaboration, *Eur. Phys. J.* **C21**, 443 (2001).

[19] E.A. Kuraev, L.N. Lipatov, V.S. Fadin, *JETP* **44**, 443 (1976); I.I. Baalitsky, L.N. Lipatov, *Sov. J. Nucl. Phys.* **28**, 822 (1978).

[20] H1 Collaboration, *Eur. Phys. J.* **C46**, 27 (2006).

[21] ZEUS Collaboration, *Eur. Phys. J.* **C52**, 515 (2007).

[22] S. Catani, M.H. Seymour, *Nucl. Phys.* **B485**, 291 (1997); Erratum: **B510**, 503 (1997).

[23] H. Jung, G.P. Salam, *Eur. Phys. J.* **C19**, 351 (2001); H. Jung, *Comput. Phys. Commun.* **143**, 100 (2002).

[24] M. Ciafaloni, *Nucl. Phys.* **B296**, 49 (1988); S. Catani, F. Fiorani, G. Marchesini, *Nucl. Phys.* **B336**, 18 (1990).

[25] H. Jung, *Comput. Phys. Commun.* **86**, 147 (1995).

[26] H1 and ZEUS Collaborations, H1prelim-08-045, ZEUS-prel-08-003.

[27] H1 Collaboration, H1prelim-07-171, August 2007.

[28] ZEUS Collaboration, contribution to the HEP2007 Europhysics Conference, Manchester, UK, July 2007.

[29] A.D. Martin, R.G. Roberts, W.J. Stirling, R.S. Thorne, *Eur. Phys. J.* **C39**, 155 (2005).

[30] S. Kretzer, H.L. Lai, F.I. Olness, W.K. Tung, *Phys. Rev.* **D69**, 114005 (2004).

[31] H1 Collaboration, *Phys. Lett.* **B528**, 199 (2002).

[32] ZEUS Collaboration, *Phys. Rev.* **D69**, 012004 (2004).

[33] B.W. Harris, J. Smith, *Phys. Rev.* **D57**, 2806 (1998).

[34] ZEUS Collaboration, ZEUS-prel-05-008-plus, July 2006.

[35] A. Meyer, contribution to the 43rd Rencontres de Moriond on QCD and High Energy Interactions 8th-15th March 2008, La Thuile, Aosta Valley, Italy.

[36] S. Frixione *et al., Nucl. Phys.* **B412**, 225 (1994); S. Frixione, P. Nason, G. Ridolfi, *Nucl. Phys.* **B454**, 3 (1995); M. Cacciari, S. Frixione, P. Nason, *JHEP* **0103**, 006 (2001).

[37] H1 Collaboration, *Phys. Lett.* **B621**, 56 (2005).

[38] H1 Collaboration, *Eur. Phys. J.* **C41**, 453 (2005).

[39] ZEUS Collaboration, *Phys. Lett.* **B599**, 173 (2004).

[40] H1 Collaboration, *Eur. Phys. J.* **C45**, 387 (2008).

[41] ZEUS Collaboration, *Eur. Phys. J.* **C49**, 511 (2007).

[42] T. Sjöstrand *et al.*, `hep-ph/0108264`.

[43] A. Gehrmann-De Ridder, T. Gehrmann, E. Poulsen, *Phys. Rev. Lett.* **96**, 132002 (2006); *Eur. Phys. J.* **C47**, 395 (2006).

[44] P.D.B. Collins, *An Introduction to Regge Theory and High Energy Physics*, Cambridge University Press, 1977.

[45] H1 Collaboration, H1prelim-06-011; *Phys. Lett.* **B638**, 422 (2006).

[46] ZEUS Collaboration, *Eur. Phys. J.* **C2**, 247 (1998).

[47] ZEUS Collaboration, *Phys. Lett.* **B487**, 273 (2000).

[48] ZEUS Collaboration, *Phys. Lett.* **B377**, 259 (1996).

[49] H1 Collaboration, *Eur. Phys. J.* **C46**, 585 (2006).

[50] ZEUS Collaboration, *Eur. Phys. J.* **C24**, 345 (2002).

[51] C. Kiesling, Proc. of the 13th International Workshop on Deep Inelastic Scattering (DIS05), Madison (WI), 2005.

[52] LEPS Collaboration, *Phys. Rev. Lett.* **91**, 012002 (2003).

[53] DIANA Collaboration, *Phys. At. Nucl.* **66**, 1715 (2003).

[54] CLAS Collaboration, *Phys. Rev. Lett.* **91**, 252001 (2003).

[55] D. Diakonov, V. Petrov, M. Polyakov, *Z. Phys.* **A359**, 305 (1997).

[56] M. Danilov, R. Mizuk, Proceedings of 19th Rencontre de Physique de la Vallee d'Aoste, La Thuile, Italy, 2007, `arXiv:0704.3531v2[hep-ex]`

[57] NA49 Collaboration, *Phys. Rev. Lett.* **92**, 042003 (2004).

[58] K. Hicks, Proceedings of the First Meeting of the APS Topical Group on Hadronic Physics, *J. Phys. Conf. Ser.* **9**, 183 (2005).

[59] ZEUS Collaboration, *Phys. Lett.* **B591**, 7 (2004).

[60] H1 Collaboration, *Phys. Lett.* **B639**, 202 (2006).

[61] H1 Collaboration, *Phys. Lett.* **B588**, 17 (2004).

[62] K. Krüger [H1 Collaboration], Proceedings of the 16th International Workshop on Deep Inelastic Scattering, University College London, April 2008.